

COMBINED XFEM-COHESIVE FINITE ELEMENT ANALYSES OF SINGLE-LAP JOINTS

FLORIN ADRIAN STUPARU, DAN MIHAI CONSTANTINESCU,
DRAGOȘ ALEXANDRU APOSTOL, MARIN SANDU, ȘTEFAN SOROHAN

Abstract. Cohesive Zone Modelling (CZM) and eXtended Finite Element Modelling (XFEM) available in Abaqus® are used together to simulate the behaviour and strength of a single-lap adhesively bonded joint. A distinct CZM model is also used. The variation of the peeling and shearing stresses in the process zone is shown and explained before and after damage initiation. Shearing and peeling stress fields along the overlap of the single-lap joint are compared by using both the XFEM-cohesive model and the cohesive model at damage initiation and propagation for two different thicknesses of the aluminium adherends. The two simulation models were tested successfully. However the XFEM-cohesive model is recommended only for particular applications. The cohesive model proved to be more accurate and easier to be used.

Key words: single-lap joint, cohesive zone model, extended finite element method, process zone, aluminium adherends.

1. INTRODUCTION

Without a better understanding of progressive failure, the fracture criteria and predictive capabilities will be limited. Interface cracking is generally a mixed mode cracking, as both normal and shear stresses develop just ahead of the crack tip [1, 2]. Experiments have shown that fracture energy can depend on mode mixity, [3–5]. A comprehensive literature review on the types of tests used for adhesive joints for single and mixed-mode fracture, underlining their advantages and disadvantages, was done by Chavez *et al.* [6]. They concluded that there is no general agreement about the test suitability for mixed-mode fracture assessment of adhesive joints.

During the crack growth process, two new surfaces are created. Before the physical crack is formed, these two surfaces are held together by traction within a cohesive zone. The traction varies in relation to the relative displacement of the surfaces, and a cohesive law describes the phenomena in the cohesive zone in

“Politehnica” University of Bucharest, Department of Strength of Materials

terms of the traction and the separation of the surfaces to be formed under the fracture process. A cohesive law is also denoted as a traction-separation law. The concept to describe the cohesive phenomena before fracture has been established for almost half a century ago. The concept of cohesive zones [7, 8] has revived interest and the cohesive zone modelling (CZM) approach has emerged as a powerful analytical tool for nonlinear fracture processes. This model considers the relation between the traction and separation that are normal to the fracture surfaces, and the unphysical stress singularity at the crack tip in the traditional linear elastic fracture mechanics is removed. The cohesive models were later extended to the mode II fracture process, in which the tangential traction and separation are considered instead. As Högberg mentions in [9], experimental observations show distinctive characteristics of the micromechanical failure mechanisms in peel and shear fracture, thus the cohesive behaviour is expected to be mode dependent [10–12].

Cohesive zone models have particularly been used to analyze composite delamination problems. Cohesive strength and fracture energy are believed to have greater importance with respect to the specific shape chosen for the cohesive model. Most damage models, such as the Progressive Damage Model for Composites provided in Abaqus[®] [13] and typical cohesive elements [14–16], represent the evolution of damage with linear softening laws that are described by a maximum traction and a critical energy release rate.

As discussed by Dávila *et al.* [16] the shape of the softening law, e.g., linear or exponential, is generally assumed to be inconsequential for the prediction of fracture for small-scale bridging conditions, but plays a fundamental role in the prediction of fracture under large-scale bridging conditions, where the process zone length may be large relative to other length scales in the problem.

FEM analyses of single-lap joints were performed in [17] using a CZM approach and allowing the cohesive properties of the interface and plastic deformation of the adherends to be included in the analysis by means of a traction–separation law with a trapezoidal shape. Using cohesive-zone parameters determined for the particular combination of materials, the numerical predictions for different bonded shapes were confirmed by the experimental observations. The numerical models predicted accurately the failure loads, displacements and deformations of the joints. Also, Campilho *et al.* [18] evaluated the tensile behaviour of adhesively bonded single-strap repairs on laminated composites as a function of the overlap length and the patch thickness. A CZM with a trapezoidal shape in pure modes I and II was used to simulate a thin ductile adhesive layer. An excellent agreement was found between the experiments and the simulations.

Cohesive laws are usually associated with cohesive zone modelling in the numerical simulation of the fracture process. Applications to material systems such as adhesively bonded joints, bimaterial interfaces, and the dynamic fracture of homogeneous materials have also been very successful.

2. XFEM AND COHESIVE ELEMENT APPROACH

The recently developed eXtended Finite Element Method (XFEM) is an extension of the FEM, and its fundamental features were described by Belytschko and Black [19], based on the idea of partition of unity presented in [20], which consists on local enrichment functions for the nodal displacements to model crack growth and separation between crack faces. With this technique, discontinuities such as cracks are simulated as enriched features, by allowing discontinuities to grow through the enrichment of the degrees of freedom of the nearby nodes with special displacement functions. As the crack tip changes its position and path due to loading conditions, the XFEM algorithm creates the necessary enrichment functions for the nodal points of the finite elements around the crack path/tip. Compared to CZMs, XFEM excels in simulating crack onset and growth along an arbitrary path without the requirement of the mesh to match the geometry of the discontinuities neither remeshing near the crack [21]. This can be an advantage to CZM modelling for the simulation of bonded engineering plastics or polymer-matrix composites, where adherend cracking may occur after initiation in the adhesive. CZM has a strong intrinsic limitation since cohesive elements to simulate damage growth must be placed at the growth lines where damage is supposed to occur. If damage would occur in another region(s), the correct results would not be provided. However, this limitation is usually of little importance as damage growth in adhesively bonded joints or structures is many times limited to typical locations such as the adhesive/adherend interfaces or within the adhesive itself. This does not occur with the XFEM, as crack propagation is allowed anywhere within the models. However, when speaking about the XFEM formulation of Abaqus[®], another drawback appears, because the prediction of damage initiation is based on one value of strength/strain which gives damage initiation (by the maximum principal stress or strain criterion, respectively). This is a limitation in the specific case of thin adhesive layers since their behaviour is not consistent with that of the corresponding bulk adhesives, because of the constraints on deformations imposed by the adherends and respective discrepancies in the stress fields near the crack tip [18].

A combined XFEM-cohesive element approach was used in [22] to model the fillet region of an aluminium–epoxy single lap joint and proved it to be highly effective. They underlined that the current implementation of XFEM and CZM in Abaqus[®] showed that there is a potential discontinuity in the crack path as at the interface the crack cannot continue in the adherend. Therefore a layer of cohesive elements in the adhesive layer was used to simulate cohesive failure at the experimentally observed site of failure.

More recently, an inverse XFEM/CZM method was proposed [23], as an experimental - numerical methodology for identification of mode I failure parameters of unidirectional fibre reinforced composites for which crack propagation is controlled by a bi-linear cohesive law. The numerically obtained critical strain

energy release rate was close to that obtained experimentally as calculated by the corrected beam theory. The agreement between the experimental and calculated strength was also good.

Comparison and evaluation of CZM and XFEM modelling, currently implemented in the FEM package Abaqus[®], to simulate the behaviour of adhesively bonded single- and double-lap joints between aluminium adherends, bonded with the brittle adhesive Araldite[®] AV138 was done [24]. The study comprises a variety of overlap lengths, between 5 and 20 mm, to test both modelling solutions under different conditions, between an approximately uniform level of shear stresses along the bond up to the large shear stress gradients found in joints with bigger bond lengths. Discussions on the capabilities and/or limitations of these two methods to model bonded structures are done by direct comparisons with experimental data.

XFEM always propagates cracks orthogonally to the maximum principal stresses/strains, which in some cases (e.g., mixed-mode damage propagation) may not correspond to the real behaviour of materials and give inaccurate predictions [24]. In these situations, the XFEM still predicts with accuracy the loci of damage initiation by the stress or strain criteria. Stress singularities that often occur in bonded structures are dealt identically to CZM modelling. Actually, stresses at singular regions never exceed σ_n^0 (normal traction at initiation), which implies the suppression of the singularity in the numerical models. Concerning the mesh dependency of the XFEM for the strength predictions, it behaves in an identical manner to CZM, since it is almost mesh independent for the simulation of fracture propagation. This is because the strain energy is averaged over a finite area (the fracture process zone) while crack growth is taking place. Thus, for a large range of mesh sizes, provided that a minimum refinement is used, all the relevant features of the failure process are accurately captured [17]. Despite this fact, given that the prediction of crack initiation is carried out by the value of σ_n^0 (in mode I), this feature is mesh dependent, as stresses/strains at concentration regions are mesh dependent as well.

This paper concentrates on describing the simultaneous use of the two simulation methods: XFEM and cohesive (CZM). As case study a single-lap joint is considered. Some results were previously presented [25]. There, the two methods were used together to simulate the behaviour and strength of a single-lap adhesively bonded joint with an initial delamination in the adhesive. Depending on the thickness of the adhesive and the position of the initial delamination, the crack initiated and propagated by XFEM changing its trajectory following the principle of local symmetry reaching or not the interface. Meanwhile failure was initiated in the cohesive elements at the interface and crack propagation continued in the same location. In this paper is analyzed the variation of the peeling and shearing stresses in the process zone before and after damage initiation by using the cohesive model. Afterwards, the shearing and peeling stress fields along the overlap are analyzed

through two models: combined XFEM-cohesive and cohesive. The aluminium adherends have the thickness of 3 mm, respectively 5 mm. The influence of the adherend thickness and the differences and similarities in using the two approaches are underlined. Some conclusions on the use of the two models are drawn.

3. COHESIVE FINITE ELEMENT MODEL

The single-lap joints used in the investigations have the geometry presented in Fig. 1. The thickness of the adhesive is kept constant to 0.5 mm and the effective overlap length is $L = 20$ mm.

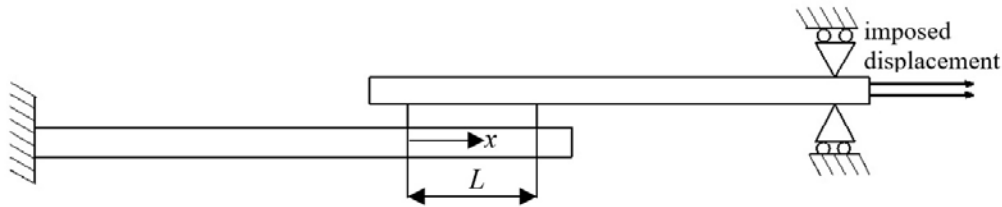


Fig. 1 – The single-lap joint geometry.

The adherends were made from aluminium. At the ends of the overlap a 5 mm gap length is kept on each side of the overlap as used to control the thickness of the adhesive layer with a wax layer of 0.5 mm, as it was done in the experimental preparation of the specimens and testing [26].

The adhesive used in the simulations is Araldite[®] 2015 (Huntsman Advanced Materials, Basel, Switzerland) with some of its mechanical properties considered as in [27] and specified in Table 1. This adhesive has a ductile behaviour. The adherends had the conventional corresponding mechanical properties are given in the same table. The considered thicknesses of the adherends were either 3 mm or 5 mm, having a width of 30 mm, and a length of 150 mm.

Table 1

Some mechanical properties of the adhesive and the adherend used in simulations

		Araldite 2015 [27]	Aluminium
Young's modulus [MPa]	E	1850	70000
Shear modulus [MPa]	G	560	26340
Normal traction at initiation [MPa]	σ_n^0	21,6	230
Shearing traction at initiation [MPa]	σ_s^0	17,9	230
Fracture energy in tension [N/mm]	G_n^c	0,43	15
Fracture energy in shear [N/mm]	G_s^c	4,70	15

As boundary conditions, one adherend was fixed at one end and on the other adherend a displacement was imposed horizontally at the opposite end.

The triangular CZM formulation was chosen for this analysis because of its simplicity, large use for investigation purposes, and availability in FEM package Abaqus® (Providence, RI, USA) including a mixed mode formulation, which is absolutely necessary to model the single-lap joints used hereby. Damage initiation can be specified by different criteria. In this work, the quadratic nominal stress criterion was selected for the initiation of damage, as previously used and tested for accuracy [26].

The two-dimensional meshing of the adhesive was done by using COH2D4 and CPE4 for adherends four-node linear plane strain elements. The adhesive layer was modelled with cohesive elements of 0.5×0.5 mm; same size of the elements was used for the adherends. In Fig. 2 the model for a 3 mm thickness adherend is shown.

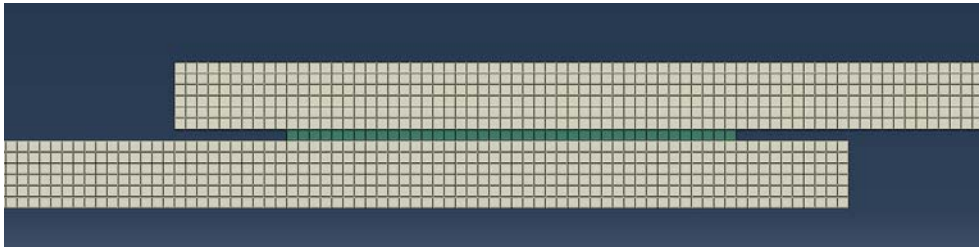


Fig. 2 – Cohesive FE model of the single-lap joint.

The variation of stresses was further represented over the length of the adhesive overlap as a function of a normalized coordinate x/L , having values from 0 to 1. Two moments were considered to be important: the initiation of damage in the first cohesive element and the moment of propagation of damage, considered as crack propagation. Damage is initiated according to the quadratic nominal stress criterion which states that the sum of the squares of the ratios between the normal and shearing stresses to their values at initiation (given in Table 1) is equal to 1.

The variation of the shearing and peeling stresses in the overlap region is significant only at the extremities of the adhesive layer. In the cohesive elements upon damage initiation the traction decreases until it reaches zero. Once the traction has become zero or, correspondingly, the damage parameter has reached 1.0 (SDEG=1 for a completely damaged cohesive element), an interfacial separation (delamination) has occurred at that material point. In Fig. 3 are shown the variation of SDEG and normalized shearing and peeling stresses to their corresponding values before damage propagation for the lap joint of 3 mm thickness and overlap length of 100 mm. The representation is done for half of the overlap length, that is up to $x/L = 0.5$.

Three distinct regions are characteristic for the damage propagation in the adhesive in the so-called *process zone*. In region I damage was already produced, tractions are zero and $SDEG = 1$; the normalized length corresponds to three cohesive elements. Region II, in front of the propagated damage (crack) is characterized by a mixed-mode loading, shearing and peeling being present. $SDEG$ decreased in this region from 1 to 0 indicating that damage is reduced in the *process zone* while the shearing stress is increasing and the peeling stress is initially tensile up to a normalized distance x/L about 0.11, then compression is produced up to $x/L = 0.22$. In the last part of the process zone, for $x/L > 0.22$ the peeling stress becomes zero and the shearing stress tends to reach its maximum value of shearing traction at initiation as the value of the normalized stresses is 1. In region III after damage initiation in shearing is produced the softening of the material gives as an effect the decrease of the shearing stress up to a constant value. Meanwhile $SDEG$ remains zero as damage is not yet produced.

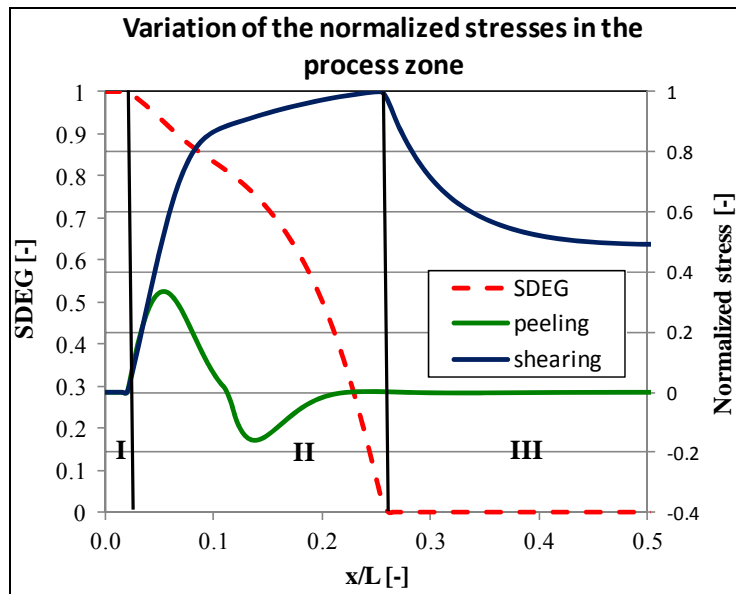


Fig. 3 – Variation of normalized stresses and damage in the process zone of the single-lap joint.

It is to be underlined once again that in the *process zone* ahead failed cohesive elements (region II) the shearing stress increases till damage initiation while the peeling stress and damage variable $SDEG$ become zero. For $x/L > 0.4$ (region III) the shearing stress is constant having a value close to the one obtained through a conventional calculus, by dividing the force to the shear area.

4. XFEM-COHESIVE FINITE ELEMENT MODEL

Both materials used for adhesive and adherends have been modelled by using the XFEM capabilities. Using this technique, damage takes place when the principal stress/strain is greater than the limit value specified in the traction-separation law. In this study a strain criterion was chosen for damage initiation and the crack propagates orthogonally to the maximum principal strain using a fracture energy criterion. The critical strain was established experimentally through traction tests as mentioned in [26]. Fracture at bonded interfaces was modelled by defining a tie constraint between the adherent and the adhesive material (local approach). The tie constraint approach allows to model zero-thickness cohesive layer using a finer discretization than that of the bulk material and may be more desirable in certain modelling situations [13]. The same material properties used for XFEM were also used for cohesive interface modelling. Only the initial stiffness value used for the cohesive elements at the interface was changed. The initially considered value was 10^6 N/mm^3 , as suggested in the literature [14], but later was diminished to 10^4 N/mm^3 as to improve the convergence issues. The zero-thickness cohesive layer damage takes place according to the quadratic nominal stress criterion and the crack propagates using power law mixed mode fracture energy behaviour.

The geometry of the single-lap joint to be analyzed with the combined XFEM-cohesive model is presented in Fig. 4. The active overlap length is $L = 20 \text{ mm}$ as before and at both ends symmetric 5 mm length delaminations were introduced in the middle of the adhesive layer of 1 mm thickness. Their role is to facilitate the initiation and propagation of damage. Imposed boundary conditions are the same as before (Fig. 1).

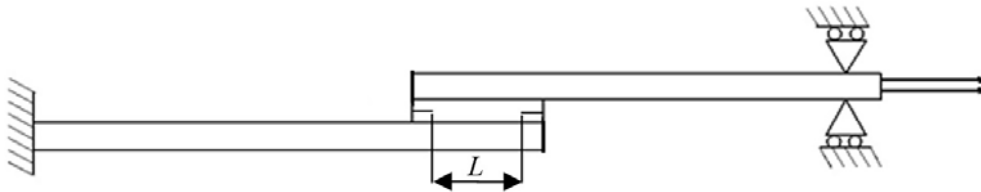


Fig. 4 – Single-lap joint geometry with lateral delaminations.

The adherends and adhesive were modelled with XFEM by using the plane strain element CPE4 of size $0.2 \times 0.2 \text{ mm}$. For optimizing the calculations the adherends were modelled with the same elements by using the *bias* function from Abaqus® which enables the increase of the size of the elements from $0.2 \times 0.2 \text{ mm}$ to $0.2 \times 1 \text{ mm}$ as to be noticed in Fig. 5. Hereby the behaviour of the adhesive and the adherends is linear elastic.

Zero-thickness cohesive elements are considered at the interface between the adhesive and the adherend.

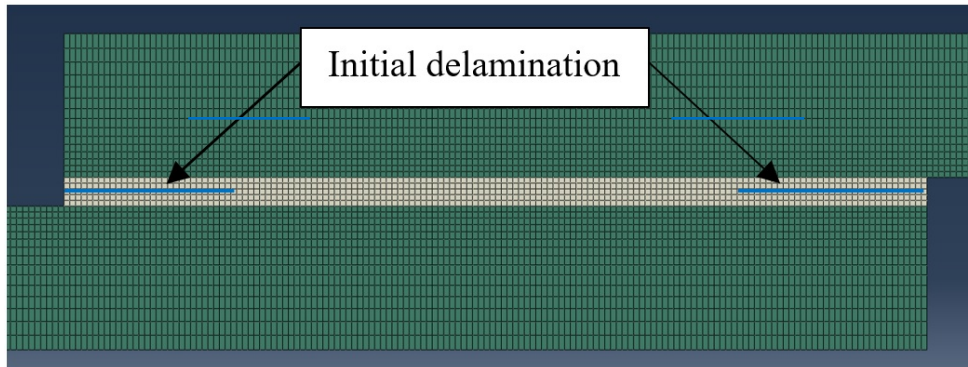


Fig. 5 – XFEM-cohesive FE model.

The force-displacement curve obtained numerically is shown in Fig. 6. The important moments are: 1 – initiation of damage (crack); 2 – propagation by XFEM through the adhesive to the interface; 3 – failure in the cohesive elements at the interface through delamination.

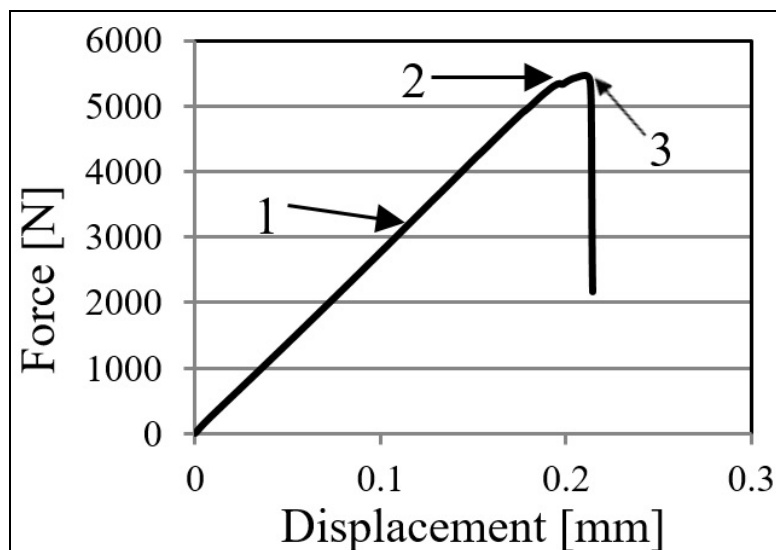


Fig. 6 – Force-displacement curve for the given geometry.

As an example, at initiation, the peeling stress and the shearing stress variations are shown in Fig. 7a, respectively Fig. 7b.

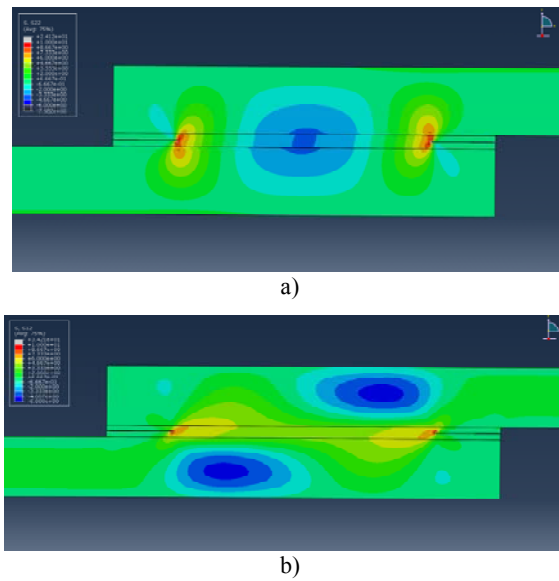


Fig. 7 – Variation of stresses at damage initiation: a) peeling stress; b) shearing stress.

When damage is propagating by XFEM and is reaching the interface, the peeling stress and the shearing stress variations are now shown in Fig. 8a, respectively Fig. 8b.

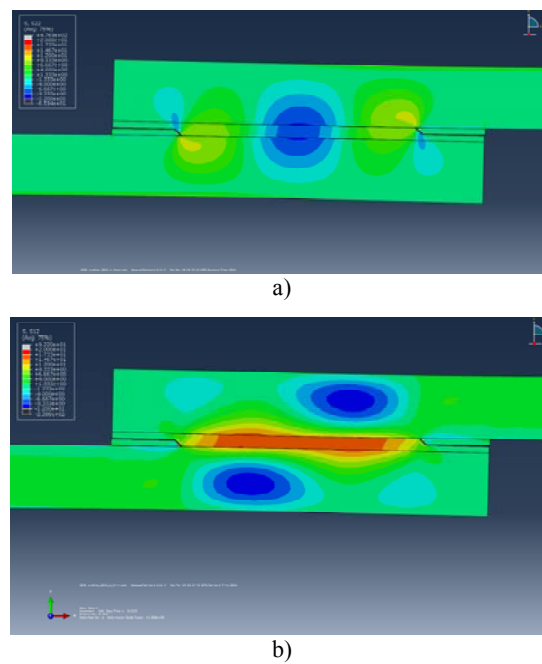


Fig. 8 – Variation of stresses at damage propagation: a) peeling stress; b) shearing stress.

After propagation the crack remains at the interface and doesn't move back to the adhesive, nor into the adherent. The XFEM is not effective any more. Cohesive elements of zero thickness take over the increase of the delamination up to the failure of the joint (point 3 in Fig. 6).

5. VARIATION OF STRESSES WITH THE XFEM-COHESIVE AND COHESIVE MODELS

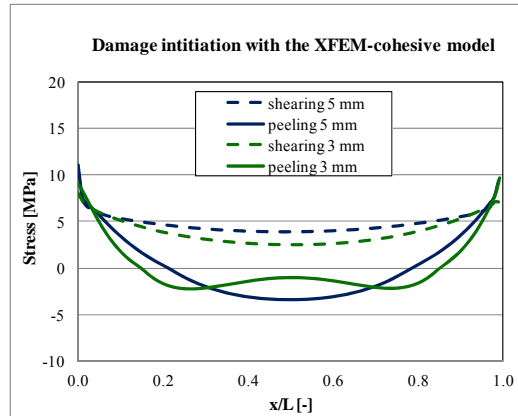
Damage initiation and propagation can be analyzed by both XFEM-cohesive and cohesive models. The first model is effective in particular situations, as seen in the previous example – crack propagating from an initial delamination. Another problem, concerning the propagation of the crack into the adherend, was also reported, [21, 24].

In order to compare the two models a pure cohesive model is established by using the same COH2D4 four-node linear plane strain elements. The adhesive layer was modelled with cohesive elements of 0.5×1 mm, as to cover with one row of elements the entire adhesive thickness. Aluminium adherends of 5 mm and 3 mm thickness are used in the joint.

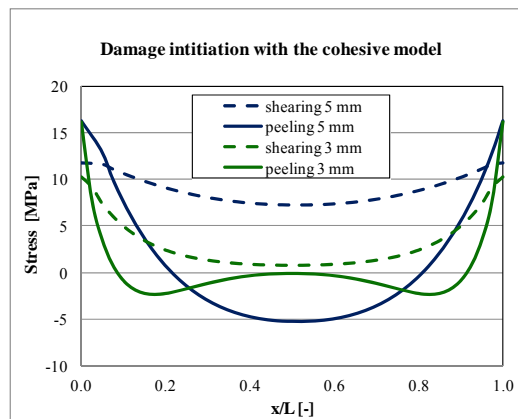
One should keep in mind that in the XFEM-cohesive model initiation is perpendicular to the maximum principal strain and in the cohesive model the quadratic nominal stress criterion takes into account both shearing and peeling.

In Fig.9 the variation of peeling and shearing stresses along the overlap length of 20 mm is shown at damage initiation for both models.

At damage initiation, in the XFEM-cohesive model, the shearing stress is almost constant over the length of the adherend regardless the adherend thickness. peeling stresses are important only at the two ends of the overlap up to $x/L = 0.15$ for 3 mm thickness and $x/L = 0.2$ for the adherend of 5 mm. By using the cohesive model a greater difference between the shearing stresses for the two thicknesses is noticed. Peeling stresses have higher values at the extremities and, again, a greater influence of the adherend thickness is to be noticed on their variation over the length of the overlap. Now the variation is important up to $x/L = 0.1$ for the thinner adherend, closer to the end of the overlap compared to the prediction obtained with the XFEM-cohesive model. For the 3 mm adherend the shearing and peeling stresses are practically zero in the middle of the overlap, for x/L between 0.4 and 0.6. For the 5 mm adherend peeling stress is negative in the middle of the overlap for $x/L > 0.2$. It is believed that the cohesive model is able to establish better the variation of both stresses at damage initiation.



a)

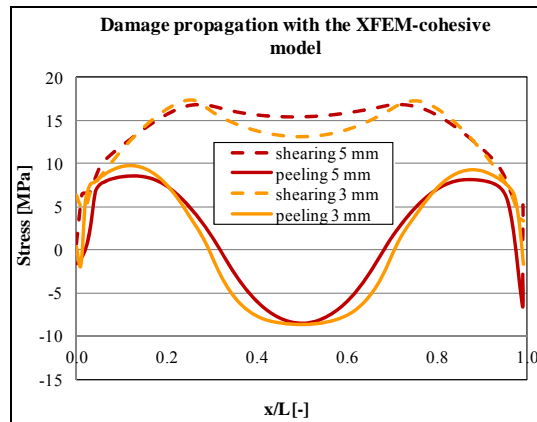


b)

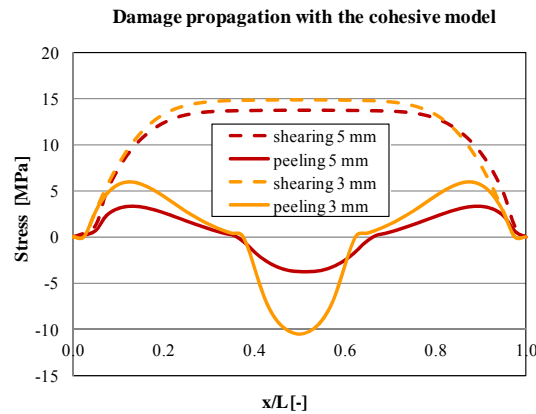
Fig. 9 – Variation of stresses at initiation in the two models: a) XFEM-cohesive; b) cohesive.

In Fig. 10 the same type of representation is done at damage propagation for both models. The shearing stress prevails for the two thicknesses regardless the model used and is mostly constant from x/L about 0.25 to 0.75. In the XFEM-cohesive model a slight decrease of this stress results in middle of the overlap.

Peeling stresses for both thicknesses show tension and afterwards compression. The XFEM-cohesive model is able to capture higher values of the peeling stress towards to extremities of the overlap, as the mesh is more refined. For both thicknesses the peeling stresses show similar variations and values. On the other hand, the cohesive model gives a steeper variation of the stresses in the compression zone for x/L between 0.4 and 0.6. For the 3 mm thickness adherend the peeling stress is in modulus greater than for the 5 mm adherend, especially for the cohesive model.



a)



b)

Fig. 10 – Variation of stresses at propagation in the two models: a) XFEM-cohesive; b) cohesive.

The stresses were determined in the third row of elements for the XFEM-cohesive model (0.2×0.2 mm) and in the one row of elements (0.5×1 mm) for the cohesive model. So, the stresses distributions are somehow averaged through the adhesive thickness. That's why the influence of the adherend thickness is not so evident. From the point of view of the boundary stress conditions at the end of the overlap the cohesive model performs better.

6. CONCLUSIONS

A cohesive model and a combined XFEM-cohesive model with zero-thickness cohesive layer are used together to better understand the state of stress in the overlap region of a single-lap adhesively bonded joint. The distinct cohesive model is used

in order to monitor the phenomena before and after damage initiation. The variation of the peeling and shearing stresses in the process zone is shown and explained in correlation to the SDEG damage parameter of the cohesive elements.

Shearing and peeling stress fields along the overlap of the single-lap joint are compared by using both the XFEM-cohesive model and the cohesive model at damage initiation and propagation. Two different thickness adherends made of aluminium were used. The XFEM-cohesive model had a more refined mesh in the adhesive and is able to capture better the stresses variations. However this model is more sensitive to issues of numerical convergence. It is recommended for simulations in applications where an initial delamination exists and its path for further propagation is of interest. The cohesive model proved to be more accurate and easier to be used. In fact the accuracy of such a model has already been demonstrated and is recommended when the path of the damage is predefined.

Acknowledgements. The authors acknowledge the support given by a grant of the Romanian National Authority for Scientific Research, CNDI-UEFISCDI, project number PN-II-PT-PCCA-2011-3.2-0068, contract 206/2012.

Received on March 7, 2016

REFERENCES

1. WILLIAMS, M.L., *The stress around a fault or crack in dissimilar media*, Bull. Seismo. Soc. Am., **49**, pp. 199–204, 1959.
2. RICE, J.R., *Elastic fracture mechanics concepts for interfacial cracks*, Trans. ASME J. Appl. Mech., **55**, pp. 98–103, 1988.
3. CAO, H.C., EVANS, A.G., *An experimental study of the fracture resistance of bimaterial interfaces*, Mech. Mater., **7**, pp. 295–304, 1989.
4. WANG, J.S., SUO, Z., *Experimental determination of interfacial toughness using Brazil-nut-sandwich*, Acta Metall., **38**, pp. 1279–1290, 1990.
5. LIECHTI, K.M., CHAI, Y.S., *Asymmetric shielding in interfacial fracture under in-plane shear*, Trans. ASME J. Appl. Mech., **59**, pp. 295–304, 1992.
6. CHAVES, F.J.P., de MOURA, M.F.S.F., da SILVA, L.F.M., DILLARD, D.A., ESTEVES, V., *Fracture Mechanics Tests in Adhesively Bonded Joints: A Literature Review*, J. Adhesion, **90**, pp. 955–992, 2014; doi: 10.1080/00218464.2013.859075
7. DUGDALE, D.S., *Yielding in steel sheets containing slits*, J. Mech. Phys. Solid., **8**, pp. 100–104, 1960.
8. BARENBLATT, G., *The mathematical theory of equilibrium cracks in brittle fracture*, Adv. Appl. Mech., **7**, pp. 55–129, 1962.
9. HÖGBERG, J.L., *Mixed mode cohesive law*, Int. J. Fract., **141**, pp. 549–559, 2006; doi:10.1007/s10704-006-9014-9
10. CHAI, H., CHIANG, M.Y.M., *A crack propagation criterion based on local shear in adhesive bonds subjected to shear*, J. Mech. Phys. Solids., **44**, pp. 669–689, 1996.
11. CHAI, H., *Interfacial mixed-mode fracture of adhesive bonds undergoing large deformation*, Int. J. Solid. Struct., **40**, pp. 6023–6042, 2003.
12. ROY, Y.A., NARASIMHAN, R., ARORA, P.R., *An experimental investigation of constraint effects on mixed mode fracture initiation in a ductile aluminium alloy*, Acta Mater., **47**, pp. 1587–1596, 1999.

13. Abaqus® 6.8. *User's Manual*, 2008. Dassault Systèmes, Providence, RI, USA.
14. CAMANHO, P.P., DÁVILA, C.G., de MOURA, M.F.S.F., *Numerical simulation of mixed-mode progressive delamination in composite materials*, J. Compos. Mater., **37**, pp. 1415–1438, 2003; doi:10.1177/0021998303034505
15. TURON, A., CAMANHO, P.P., COSTA, J., DÁVILA, C.G., *A damage model for the simulation of delamination in advanced composites under variable-mode loading*, Mech. Mater., **38**, 1072–1089, 2006; doi:10.1016/j.mechmat.2005.10.003
16. DÁVILA, C.G., ROSE, C.A., CAMANHO, P.P., *A procedure for superposing linear cohesive laws to represent multiple damage mechanisms in the fracture of composites*, Int. J. Fract., **158**, pp. 211–223, 2009; doi:10.1007/s10704-009-9366-z
17. KAFKALIDIS, M.S., THOULESS, M.D., *The effects of geometry and material properties on the fracture of single lap-shear joints*, Int. J. Solids Struct., **39**, pp. 4367–4383, 2002; doi:10.1016/S0020-7683(02)00344-X
18. CAMPILHO, R.D.S.G., de MOURA, M.F.S.F., DOMINGUES, J.J.M.S., *Using a cohesive damage model to predict the tensile behaviour of CFRP single-strap repairs*, Int. J. Solids Struct., **45**, pp. 1497–1512, 2008; doi:10.1016/j.ijsolstr.2007.10.003
19. BELYTSCHKO, T., BLACK, T., *Elastic crack growth in finite elements with minimal remeshing*, Int. J. Fract., **45**, pp. 601–620, 1999.
20. MELENK, J.M., BABUSKA, I., *The partition of unity finite element method: basic theory and applications*, Seminar für Angewandte Mathematik, Eidgenössische Technische Hochschule, Research Report No. 96-01, January, CH-8092 Zurich, Switzerland, 1996.
21. CAMPILHO, R.D.S.G., BANEIA, M.D., CHAVES, F.J.P., da SILVA, L.F.M., *eXtended Finite Element Method for fracture characterization of adhesive joints in pure mode I*, Comput. Mater. Sci., **50**, pp. 1543–1549, 2011; doi:10.1016/j.commat.2010.12.012
22. MUBASHAR, A., ASHCROFT, I.A., CROCOMBE, A.D., *Modelling Damage and Failure in Adhesive Joints Using A Combined XFEM-Cohesive Element Methodology*, J. Adhesion, **90**, 682–697, 2014; doi: 10.1080/00218464.2013.826580
23. BOUHALLA, L., MAKRAFI, A., BELOUETTAR, S., YOUNES, A., NATARAJAN, S., *An XFEM/CZM based inverse method for identification of composite failure parameters*, Comput. Struct., **153**, pp. 91–97, 2015; doi: 10.1016/j.compstruc.2015.02.035
24. CAMPILHO, R.D.S.G., BANEIA, M.D., PINTO, A.M.G., da SILVA, L.F.M., de JESUS, A.M.P., *Strength prediction of single-and double-lap joints by standard and extended finite element modelling*, Int. J. Adhes. Adhes., **31**, pp. 363–372, 2011; doi: 10.1016/j.ijadhadh.2010.09.008
25. STUPARU, F.A., CONSTANTINESCU, D.M., APOSTOL, D.A., SANDU, M., *A combined cohesive elements – XFEM approach for analyzing crack propagation in bonded joints*, J. Adhesion, **92**(7-9), pp. 535–552, 2016; doi: 10.1080/00218464.2015.1115355
26. STUPARU, F.A., APOSTOL, D.A., CONSTANTINESCU, D.M., SANDU, M., SOROHAN, S., *Failure analysis of dissimilar single-lap joints*, Frattura ed Integrità Strutturale, **36**, pp. 70–78, 2016; doi: 10.3221/IGF-ESIS.36.08
27. CAMPILHO, R.D.S.G., BANEIA, M.D., NETO, J.A.B.P., da SILVA, L.F.M., *Modelling of single-lap joints using cohesive zone models: effect of the cohesive parameters on the output of the simulations*, J. Adhesion, **88**, pp. 513–533, 2012; doi: 10.1080/00218464.2012.660834.